

Evaluation of Liquefaction Potential of Soils

T.G.Sitharam

*Professor, Department of Civil Engineering, Indian Institute of Science, Bangalore
sitharam@civil.iisc.ernet.in*

1.0 Introduction

It is widely recognized that earthquakes are among the most severe natural disasters causing significant damages such as failure of earth structure, settlement or tipping of buildings, lateral spreading of sloping ground and densification causing vertical settlements. The reasons for these failures can be attributed either due to the compaction of loose deposits of soils or by a phenomenon called liquefaction. The phenomenon of liquefaction is associated with a condition of zero effective stress due to progressive increase in pore water pressure resulting from the tendency to densification of the sand structure subjected to cyclic loading. The generation of excess pore pressure under undrained loading condition is a hallmark of all liquefaction phenomena. The relative incompressibility of the pore water makes the rapid compaction of the sand impossible. Instead, an excess pore water pressure develops whose value increases with the duration of cyclic loading and many a time these pressures only start dissipating after the ground shaking has ended. Due to its high potential to cause damages, this phenomenon of liquefaction during earthquakes has become a prime subject of concern in the geotechnical engineering. Catastrophic failures in recent earthquakes have provided a serious reminder that liquefaction of sandy soils and sands with large amount of non-plastic fines as a result of earthquake ground shaking poses a major threat to the safety of civil engineering structures. Primary seismological factors that control liquefaction are amplitude and frequency of the cyclic shear stress besides the duration of shaking. Whereas, the other site-specific factors that control development of liquefaction of soil are grain size distribution of the soil mass, relative density of the soil deposit, depth and thickness of different soil strata, depth of ground water table etc. Major landslides, lateral spreads, settling and tilting of buildings and failure of waterfront retaining structures were some of the observed excellent examples of liquefaction triggered by the recent Bhuj earthquake on 26th January 2001. In many places of earthquake-affected area several sand boils/water fountains (Figure 1) were developed indicating the occurrence of extensive liquefaction.

2.0 Factors Controlling Liquefaction

In the recent past, a qualitative understanding from laboratory investigation on the liquefaction process, pore water pressure generation and post liquefaction behaviour in sandy soils has considerably enhanced by various researchers (Seed and Lee 1966; Peacock and Seed, 1968; Ishihara et al 1975; Finn et al., 1981; Dobry et al., 1982; Li et al 1988; Hyodo et al., 1994; Toyota et al., 1995; Talaganov, 1996; Vaid and Thomas, 1997; GovidaRaju, 2005). Many factors govern the liquefaction process for in situ soil and the the most important are intensity of earthquake and its duration, location of ground water table, soil type, soil relative density, particle size gradation, particle shape, depositional environment of soil, soil drainage conditions, confining pressures, aging and cementation of the soil deposits, historical environment of the soil deposit and building/additional loads on these deposits. Figure 2a (Xenaki and Athanasopoulos, 2003) shows two sets of grain size curves showing the ranges of grain size distribution for most liquefiable and potentially liquefiable soils in geotechnical criterion. In summary, the site conditions and soil type that are most susceptible to liquefaction are given in the following sections. Figure 2b shows the grain size distribution curves of the soils tested (Sands from Assam, Bhuj and Ahmedabad) along with the boundaries of most liquefiable soils.

2.1 Site Conditions

- Site that is close to the epicenter of fault rupture of a major earthquake
- Site that has a ground water table close to ground surface

2.2 Soil Type Most Susceptible to Liquefaction for Given Site Conditions

- Sand that has uniform gradation and rounded particles, very loose density state, recently deposited with no cementation between soil grains, and no prior preloading or seismic shaking



Figure 1 A typical site showing extensive Liquefaction

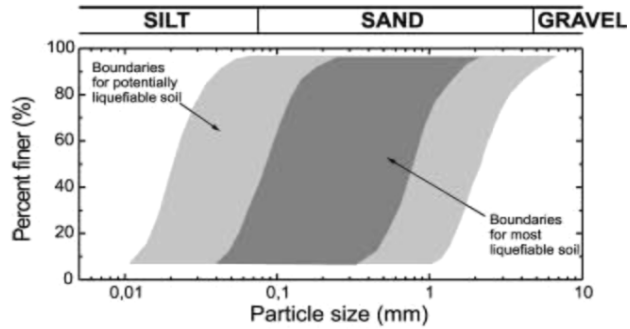


Figure 2a Range of grain size distribution for liquefaction susceptibility of soils

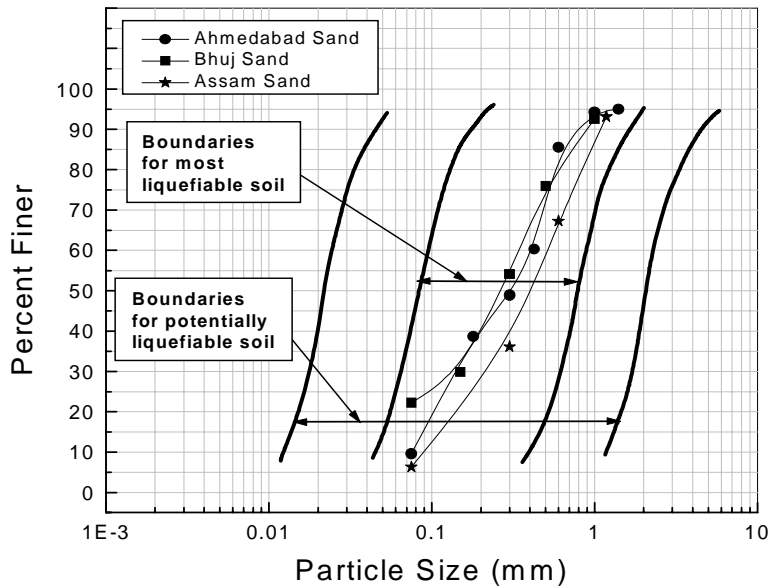


Figure 2b Grain Size distribution of soils tested

3.0 Methods To Evaluate Liquefaction Potential Of Soil

Several approaches to evaluate the potential for liquefaction have been developed. The commonly employed are cyclic stress approach and cyclic strain approach to characterize the liquefaction resistance of soils both by laboratory and field tests. The cyclic stress approach to evaluate

liquefaction potential characterizes both earthquake loading and the soil liquefaction resistance in terms of cyclic stresses. But, in the cyclic strain approach, earthquake loading and liquefaction resistance are characterized by cyclic strains. Cyclic triaxial test, cyclic simple shear test and cyclic torsional shear test are the common laboratory tests. Further, Standard Penetration Test, cone Penetration Test, Shear wave velocity method, Dilatometer test are some of the insitu tests to characterize the liquefaction resistance. Even though, cyclic stress and cyclic strain approaches are most widely used in the field of geotechnical earthquake engineering, some other approaches such as Energy dissipation, Effective stress based response analysis and Probabilistic approaches have been also developed. Figure 3 presents a chart (developed by Seed et al. 1985) that can be employed to determine the cyclic resistance ratio of the in situ soil. This chart was developed from observations and investigations of numerous sites that had liquefied and did not liquefy during the earthquakes.

Figures 4 and 5 can be used to evaluate the cyclic resistance ratio of in situ soil using cone penetration test data for clean sands & silty sands and clean gravels & silty gravels respectively. This method is an alternative to standard penetration test in which the corrected CPT tip resistance q_{c1} is used.

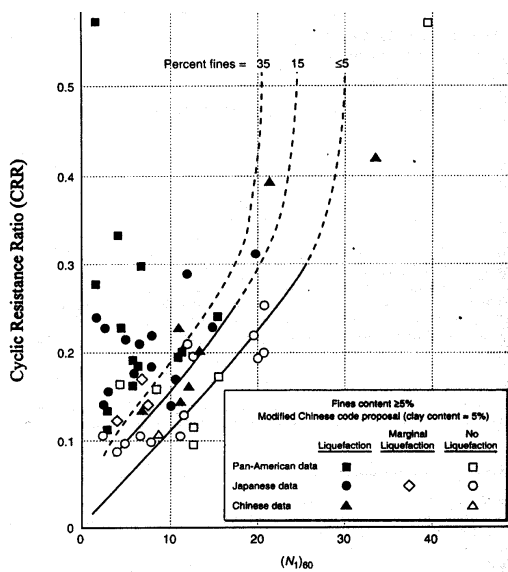


Figure 3 Cyclic resistance ratio causing liquefaction and $(N_1)_{60}$ values for magnitude 7.5 earthquake for clean sands and silty sands

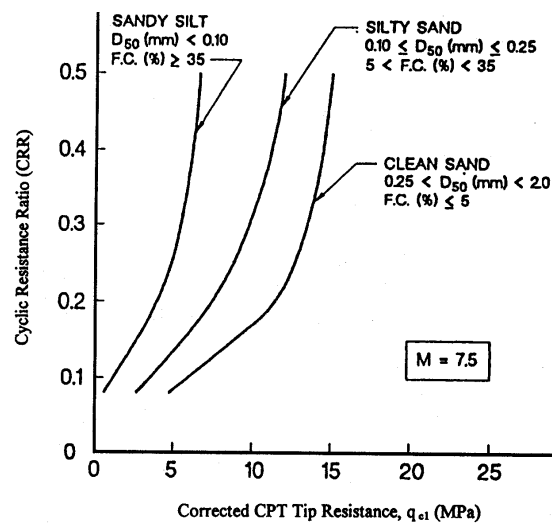


Figure 4 Cyclic resistance ratio causing liquefaction and corrected CPT tip resistance values for magnitude 7.5 earthquake for clean sands and silty sands

Figure 6 presents a chart for evaluating the liquefaction resistance of the in situ soil based on the measured shear wave velocity of the soil. The shear wave velocity can be measured in situ employing different geophysical techniques, such as the uphole, down-hole, or cross-hole methods. Here, v_{s1} represents the corrected shear wave velocity.

The seismic piezo-cone (figures 7a and b) is a prospective in-situ tool to directly evaluate soil liquefaction potential of the ground. The development of seismic piezo-cone is carried out jointly with M/s HEICO, NewDelhi. IISc has supplied the technical details and M/s HEICO has implemented the same in their existing static piezo-cone system. The developed seismic piezo-cone is calibrated at IISc in the calibration chamber of 2m \times 2m (6 feet height \times 6 feet diameter) under controlled laboratory

model tests. The seismic piezo-cone consists of a cone penetrometer coupled with a hydraulic shaker to induce liquefaction locally in the vicinity of probe during penetration at desired depth. The seismic piezo-cone has three built-in sensors: (1) Load cell for tip resistance, (2) load cell for skin resistance, (3) Piezo sensor for pore pressure measurement. The geometry of the piezocone is as shown in the figure 2 (the vibrator is located just above the cone). The cone has a projected cone area of 10 cm², a friction sleeve area of 150 cm², and a cone apex angle of 60°. Both the tip and sleeve load cell calibration showed zero return, excellent linearity, practically no hysteresis, and high repeatability. The cone has a provision for vibration with sinusoidal wave form upto a frequency range of 1 to 10HZ. This is done through a coupled hydraulic actuator at the top of the cone. This peizovibrocone can be used for evaluation of site liquefaction. Figure 7c shows a field test in progress.

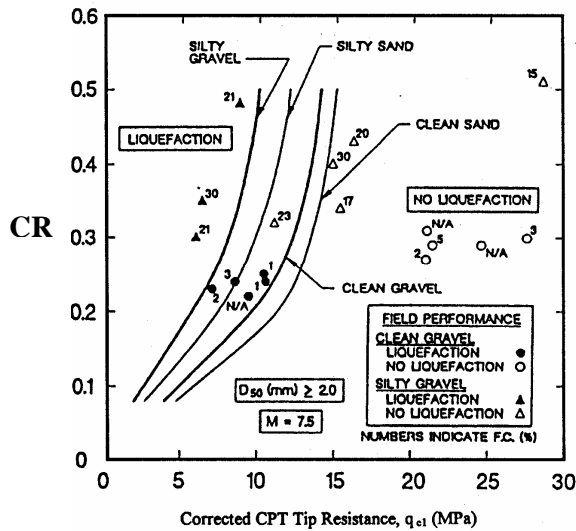


Figure 5 Cyclic resistance ratio (CRR) and corrected CPT tip resistance values for magnitude 7.5 earthquake for clean gravels and silty gravels

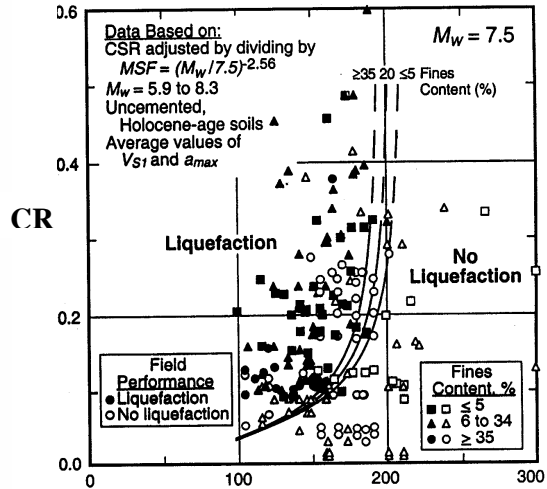


Figure 6 Cyclic resistance ratio (CRR) causing liquefaction and shear wave velocity for clean sand and silty sand

4.0 Experimental Investigation

The state-of-the-art cyclic triaxial testing facility (figure 7d), installed in geotechnical engineering division of Indian Institute of Science, Bangalore with the financial support from Department of Science and Technology (Seismology division), Govt. of India, New Delhi, is used to study the behavior of soils subjected to dynamic loading, liquefaction behaviour and also to estimate the dynamic soil properties such as shear modulus (G) and damping (D) required for design of geotechnical structures subjected to earthquake loading. The system is completely automated and computerized, which consists of servo-controlled submersible load cell (with a capacity of 10 kN) and an hydraulic actuator with frequency range of 0.01Hz to 10 Hz for applying vertical dynamic loading on the sample. The triaxial cell has the facility to conduct the tests on soil samples of sizes 38mm, 50mm, 75mm and 100mm diameter with confining pressures up to 1000 kPa using pneumatic control panel. Both stress-controlled and strain-controlled tests can be performed using built in sine, triangular and square waveforms or any other desired loading waveform by means of external input. The axial deformation, lateral deformation, volume change, cell pressure, cyclic load and sample pore water pressure can be monitored using a built-in data acquisition system. Series of tests have been carried

out to characterize the dynamic properties of liquefied sands from Bhuj (close to epicenter), from sand dykes during 1950 Assam Earthquake, and also sands from Ahmedabad (for details see GovindaRaju 2005, Ravishankar 2006, Vinod 2006).



Figure 7a Cone penetrometer system

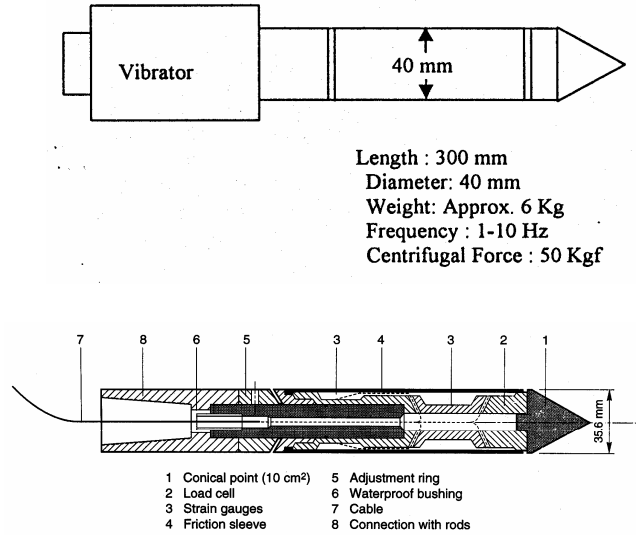


Figure 7b. Seismic Piezo cone



Figure 7c CPT test in progress

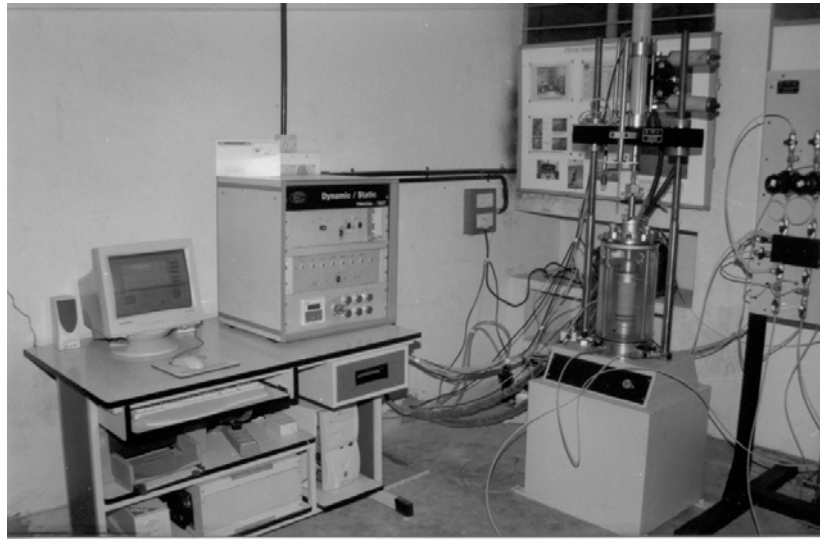


Figure 7d *Cyclic Triaxial testing Facility*

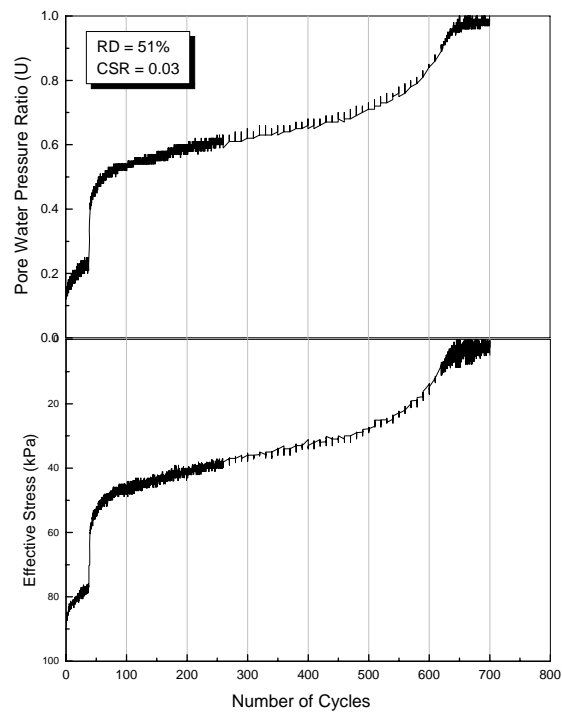


Figure 8 *Variation of Pore water pressure ratio and Effective Stress with cycles*

5.0 Evaluation Of Liquefaction Potential Of Soils

Figures 8 and 9 illustrate the typical results of the stress-controlled cyclic tests carried out on sand samples from Bhuj. It is evident from figure 8 that, for the soil sample prepared at relative density (RD) 51%, the pore water pressure builds up steadily as the cyclic axial stress ($CSR = 0.03$) is applied, and eventually approaches a value equal to the initially applied confining pressure (cyclic pore pressure ratio = 1) in 645 cycles of loading. The increase in pore water pressure results in a corresponding decrease in the effective stress, which finally reduces to zero when the pore water pressure ratio is equal to one. This stage corresponds to a double amplitude axial strain of 5% (Figure 9). Such a state of the specimen is recognised as "liquefaction" (as defined by Ishihara, 1993), which is a state of softening produced suddenly with the complete loss of shear strength or stiffness. Further, it is evident from figure 9 that, as the constant-amplitude cyclic axial stress is applied to the soil specimen having a medium density (RD = 51%) there is a sudden and rapid increase in axial strain as high as 20%. Thus, once the sandy soil having a medium density liquefies, there is significant increase in the axial strain.

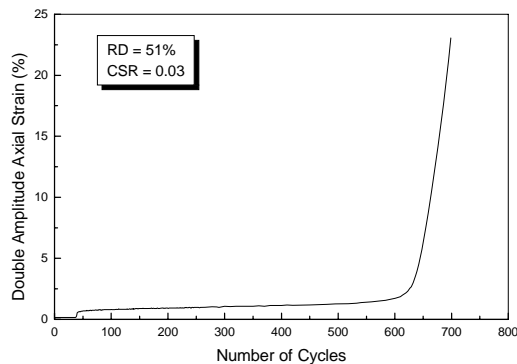


Figure 9 Variation of double amplitude axial strain with cycles

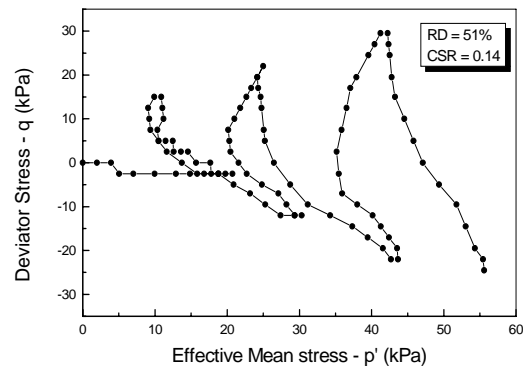


Figure 10 Stress path

Figure 10 shows the stress path during the application of constant-amplitude cyclic axial stress ($CSR = 0.14$). It can be noticed from the figure that there is a permanent loss in the shear strength as the stress path moves to the left with decreasing value of effective stress. Here the soil liquefied in five cycles of uniform load applications at a cyclic stress ratio of 0.14. The data shown in the plot is from the second cycle.

Similar undrained response of the soil sample prepared at relative density of 60% can be observed as in Figures 11. For this state of the soil, the pore water pressure ratio also becomes equal to 1.0 during the application of cyclic axial stress. At cyclic stress ratio of 0.082, the soil liquefies in 40 cycles of constant-amplitude cyclic axial stress (with small residual shear strength of about 5 kPa).

Figure 12 shows the plot of double amplitude axial strain with number of cyclic loadings. In this case, as the soil becomes dense (compared to relative density of 51%), there is no sudden increase in the axial strain, but the axial strain slowly increases with applications of cyclic axial stress. This is because, due to the reversal of the cyclic axial stress, dense sand tends to dilate, resulting in an increased undrained shear resistance. Even though, dense sands do not reach a liquefaction state (cyclic pore pressure ratio, $U = 1$), it is only a momentary condition. Hence, this state is referred to as cyclic mobility in which the soil may only momentarily liquefy with a limited undrained deformation.

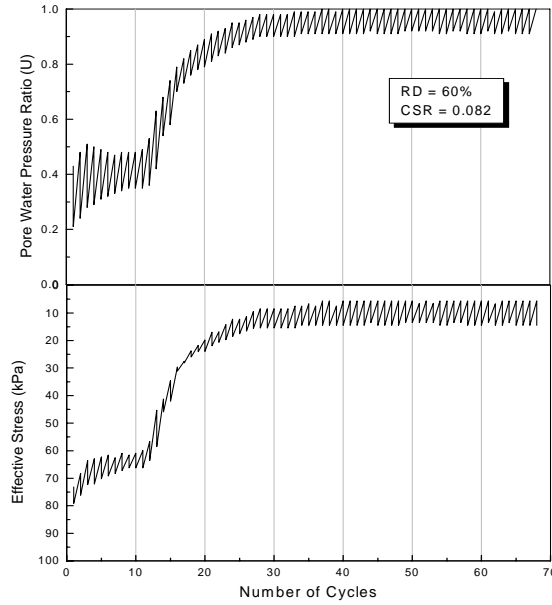


Figure 11 Variation of Pore water pressure ratio and Effective Stress with cycles

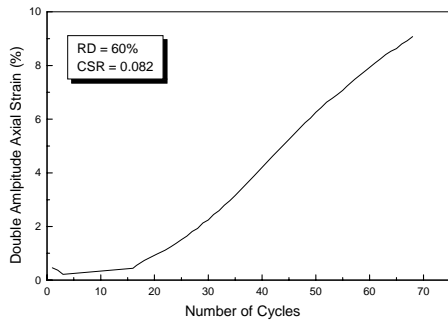


Figure 12 Variation of double amplitude axial strain with cycles

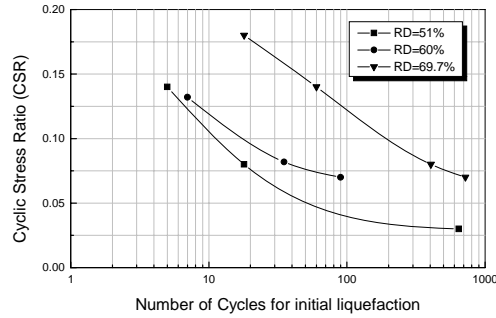


Figure 13 Liquefaction resistance curves for Bhuj sand

Figure 13 shows the cyclic resistance curves of the sand tested at three different relative densities. The cyclic strength of sand is specified in terms of the magnitude of cyclic stress ratio required to produce 5% double amplitude axial strain in 20 cycles of constant-amplitude cyclic axial stress (as described by Ishihara, 1993). The cyclic strengths obtained are 0.075, 0.09 and 0.182 for soil samples at relative densities 51%, 60% and 69.7% respectively. It is evident from the results that for the sand having the same effective confining pressure, denser the soil, the greater the resistance to liquefaction. Thus, a dense soil will require a higher cyclic deviator stress or more cycles of deviator stress to cause liquefaction, as compared to the same soil in a loose state.

The potential for liquefaction of Ahmedabad sand has been evaluated in the cyclic strain approach in a manner similar to that used in the cyclic stress approach for a soil sample at relative density of 30%. The specimens were subjected to sinusoidal cyclic loading with cyclic shear strain of constant amplitude in the range of 0.15% to 3.4% under an effective confining pressure of 100 kPa with 1 Hz frequency. Figure 14 presents the results of a strain –controlled cyclic triaxial test on the soil.

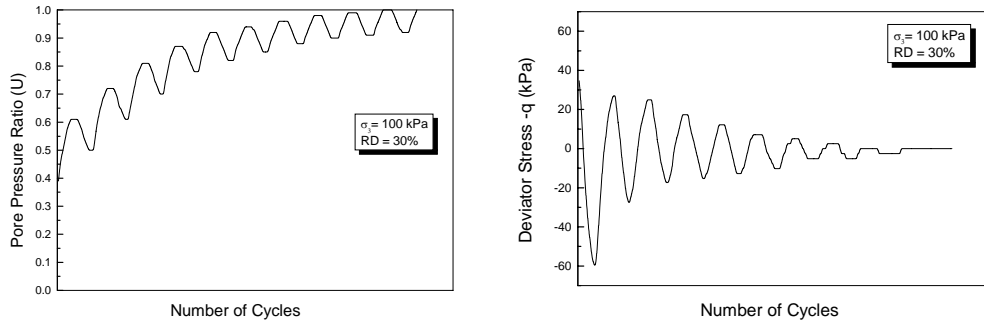


Figure 14 Variation of pore pressure ratio and deviator stress with number of cycles

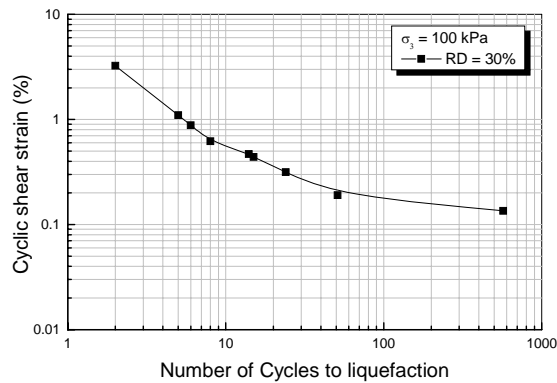


Figure 15 Liquefaction resistance curve for Ahmedabad sand

As shown in the figure 14, there is a sudden build up of pore water pressure in the first cycle itself and there after increases steadily. The 100% pore pressure ratio occurs in 10th cycle at which the deviator stress reduces to zero indicating the stage of liquefaction of soil. Figure 15 shows the liquefaction resistance curve of the Ahmedabad sand tested. As the amplitude of shear strain increases, the number of strain cycles to trigger liquefaction decreases. Here, the cyclic loading imposed by the earthquake, characterized by the amplitude of a series of uniform strain cycles, is compared with the liquefaction resistance, which is expressed in terms of the cyclic strain amplitude required to initiate liquefaction in the same number of cycles.

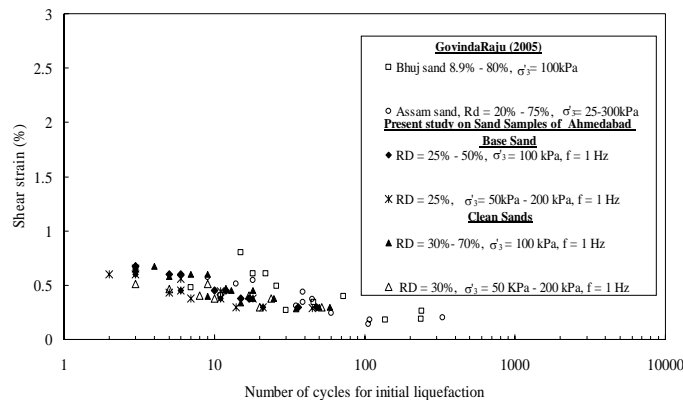


Figure 16 Relationship between shear strain and number of cycles for initial liquefaction for different parameters

Figure 16 shows the relationship between shear strain and number of cycles for initial liquefaction for base sand (9.2% silt content) and clean sand for wide range of relative densities and confining pressures. Also presented in this figure the results of strain controlled cyclic triaxial testing for wide range of relative density and confining pressures as reported by GovindaRaju (2005). As it can be observed from the figure 16 all the value are falling in a narrow range highlighting the fact that the influence of relative density, confining pressure and presence of 9.2% of silt content in the base sand samples has no significant influence on the liquefaction potential. These results are in good agreement with the experimental finding of Talaganov (1996).

The combined relationship between the pore pressure and the cycle ratio for base sand, clean sand samples for wide range of relative densities, confining pressures and clean sands with different percentage of non-plastic fines is shown in the figure 17. As it can be seen from the figure that all the values of the present study fall in a small band for a wide range of shear strain amplitudes, relative densities, confining pressures or the silt content in the sand samples. This clearly indicates that the behaviour is unique in the generation of pore water pressure with number of loading cycles. Similar trend of results have been reported by Talaganov (1996) and GovindaRaju (2005) for a wide range of parameters. The results of the present study are compared with the range as given by that of Talaganov (1996) for wide range of relative densities, confining pressures and strain amplitudes. The results of the present study fall very close to the lower bound curve of Talaganov (1996).

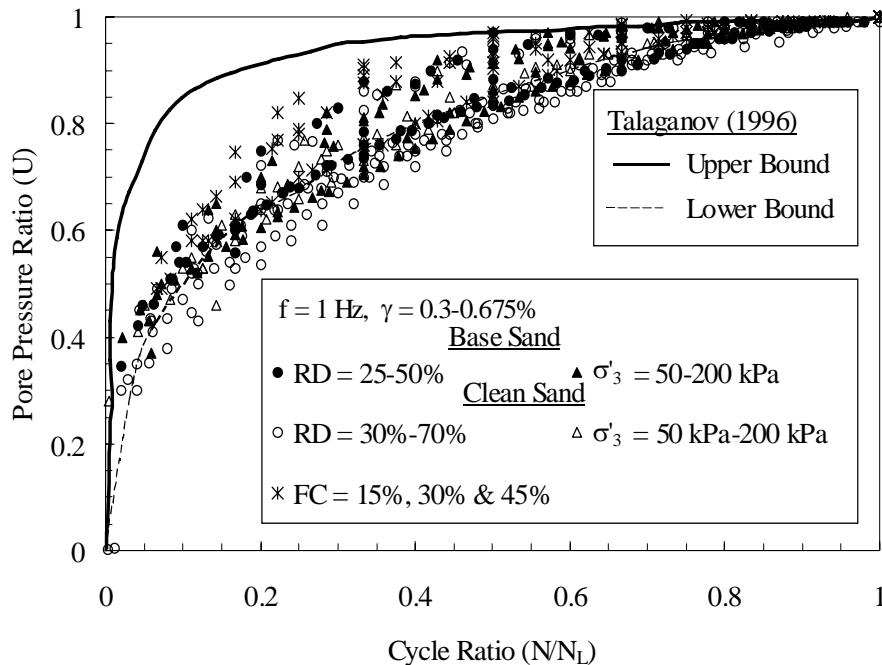


Figure 17 Relationship between pore pressure ratio and cycle ratio for sand samples for different parameters

Figure 18 shows the pore pressure ratio as a function of shear strain for base sand (with 9.2% silt) and clean sand for wide range of relative densities and confining pressures corresponding to ten numbers of cycles. Also shown in this figure is the lower and upper bound curves proposed by Dobry (1985) for ten numbers of loading cycles. As seen from the figure despite slight scatter in the data of the present study, the results of pore pressure ratio corresponding to ten cycles plots with in the band as proposed by Dobry (1985).

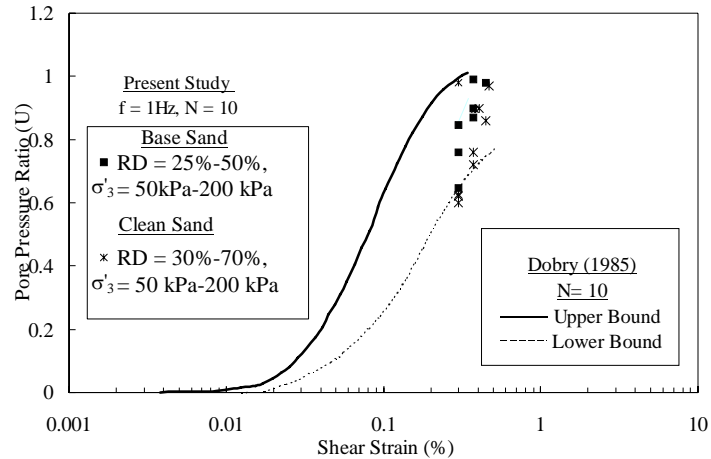


Figure 18 Variation of pore pressure ratio with shear strain at ten cycles

6.0 Concluding Remarks

Both stress-controlled and strain-controlled cyclic triaxial compression tests were conducted on the sand samples collected from Assam, Bhuj and Ahmedabad locations. Experimental investigation highlights that the potential for liquefaction of the sandy soils depends on the strain amplitude, initial relative density and initial effective confining pressure. A tendency to establish a unique relationship irrespective of initial confining pressure, relative density and strain amplitude has been observed. Pore water pressure build up as a function of cyclic shear strain amplitude of sands for different relative densities, confining pressures corresponding to ten cycles of loading compare well with in the lower and upper bounds as proposed by Dobry (1985). The results of the present study on pore water pressure build up during cyclic loading for wide range of relative densities, confining pressures and strain amplitudes fall very close to the lower bound curve of Talaganov (1996). The potential for liquefaction (or cyclic mobility) of these soils containing a large amount of fines are evaluated. As a result of application of cyclic loads on these soils, pore water pressure builds up steadily and reach initially applied confining pressure depending up on the magnitude of cyclic stress ratio as well as the density of the soil. At higher cyclic stress ratios, the pore water pressure builds up fast and there is triggering of liquefaction at lower cycles of uniform load applications. An increase in the density results in an increase in the cyclic strength of the soil there by making it less susceptible to liquefaction. The amplitude of cyclic shear strain governs the liquefaction resistance of a soil characterized by the cyclic strain approach. The resistance of soil to liquefaction decreases with increasing number of cyclic shear strains.

7.0 References

1. ASTM Designation: D 5311-92 (Reapproved 1996) Standard Test Method for Load Controlled Cyclic Triaxial Strength of Soil, Annual Book of ASTM standards, Vol. 04.08
2. ASTM Designation: D 3999-91 Standard Test Methods for the Determination of the Modulus and Damping Properties of Soils using the Cyclic Triaxial Apparatus, Annual Book of ASTM standards, Vol. 04.08
3. Braja M.Das, Vijay K. Puri and Shamsheer Prakash "Liquefaction of silty soils", *Earthquake Geotechnical Engineering*, Seco e Pinto (ed), Balkema, Rotterdam, 1999, pp619-623.
4. Dobry, R. (1985). Liquefaction of soils during earthquakes, Committee on Earthquake Engineering, Commission on Engineering and Technical Systems, National Research Council, National Academy Press, Washington, D.C.

5. Dobry, R., Ladd, R.S., Chang, R.M. and Powell, D. (1982). Prediction of pore water pressure build up and liquefaction of sands during earthquakes by the cyclic strain method, NBS Building Science Series 138, Washington, DC, pp.1-150.
 6. K.Ishihara, " Liquefaction and flow failure during earthquake", *Geotechnique*, 106, No 3, 1993, pp.351-415.
 7. Steven L. Kramer, *Geotechnical earthquake engineering*, Prentice Hall International Series, 1996.
 8. Talaganov, K. V. (1996), Stress-strain transformations and liquefaction of sands, *Soil Dynamics and Earthquake Engineering*, No.15, pp. 411-418.
 9. Xenaki V.C. and Athanasopoulos G.A. " Liquefaction resistance of sand-mixtures: an experimental investigation of the effect of fines" *Soil Dynamics and Earthquake Engineering*, No.23, 2003, pp.183-194.
 10. Finn, W. D. L. (1981). Liquefaction Potential: Development since 1976. Proceedings of the First International Conference on Recent Advances in Geotechnical Engineering and Soil Dynamics, St. Louis, Vol. 2, pp. 655 -681.
 11. GovindaRaju, L. (2005), Liquefaction and dynamic properties of sandy soils, Ph.D. thesis, submitted to Indian Institute of Science, Bangalore, India
 12. Hyodo, M, Tanizizu, H, Yasufuku, N. and Hidfkazu, M (1994), Undrained cyclic and monotonic triaxial behaviour of saturated loose sands, " *Soils and Foundations*, Vol. 134, No1. pp. 19 -32.
 13. Ishihara,K., Tatsuoka, F. and Yasuda, S. (1975), Undrained deformation and liquefaction of sand under cyclic stresses, *Soils and Foundations*, Vol.15, No.1, pp.29-44.
 14. Seed, H. B and Lee, K. L (1966), Liquefaction of saturated sands during cyclic loading, *Journal of Soil Mechanics and Foundation Division, ASCE*, Vol.92; No SM6, pp.105-134.
 15. Ravishankar, B. (2006) Cyclic and monotonic undrained behaviour of sandy soils, Ph,D, Thesis, Indian Institute of Science, Bangalore.
 16. Vinod.J.S. (2006) Liquefaction and dynamic properties of granular materials: A Discrete element approach, Ph,D, Thesis, Indian Institute of Science, Bangalore.
-